Cell Reports
Article

Specificity of Monosynaptic Sensory-Motor Connections Imposed by Repellent Sema3E-PlexinD1 Signaling

Kaori Fukuhara,[1,6] Fumiyasu Imai,[1,6] David R. Ladle,[2] Kei-ichi Katayama,[1] Jennifer R. Leslie,[1] Silvia Arber,[3,4] Thomas M. Jessell,[5] and Yutaka Yoshida[1,*]
[1]Division of Developmental Biology, Cincinnati Children's Hospital Medical Center, Cincinnati, OH 45229, USA
[2]Department of Neuroscience, Cell Biology, and Physiology, Wright State University, Dayton, OH 45435, USA
[3]Biozentrum, Department of Cell Biology, University of Basel, 4056 Basel, Switzerland
[4]Friedrich Miescher Institute, 4058 Basel, Switzerland
[5]Howard Hughes Medical Institute, Departments of Neuroscience and Biochemistry and Molecular Biophysics, Kavli Institute for Brain Science, Columbia University, New York, NY 10032, USA
[6]These authors contributed equally to this work
*Correspondence: yutaka.yoshida@cchmc.org
http://dx.doi.org/10.1016/j.celrep.2013.10.005

SUMMARY

In mammalian spinal cord, group Ia proprioceptive afferents form selective monosynaptic connections with a select group of motor pool targets. The extent to which sensory recognition of motor neurons contributes to the selectivity of sensory-motor connections remains unclear. We show here that proprioceptive sensory afferents that express *PlexinD1* avoid forming monosynaptic connections with neurons in *Sema3E*$^{+}$ motor pools yet are able to form direct connections with neurons in *Sema3E*^{off} motor pools. Anatomical and electrophysiological analysis of mice in which Sema3E-PlexinD1 signaling has been deregulated or inactivated genetically reveals that repellent signaling underlies aspects of the specificity of monosynaptic sensory-motor connectivity in these reflex arcs. A semaphorin-based system of motor neuron recognition and repulsion therefore contributes to the formation of specific sensory-motor connections in mammalian spinal cord.

INTRODUCTION

The strategies and mechanisms that confer synaptic specificity in the vertebrate CNS remain poorly defined. One strategy for constraining connections appears to involve the spatially ordered settling position of neurons (Sürmeli et al., 2011; Tripodi et al., 2011; Zlatic et al., 2009). The dorsoventral settling positioning of motor neurons has been shown to influence the specificity of sensory inputs in the developing spinal cord through a motor neuron-independent set of sensory-targeting signals (Sürmeli et al., 2011). Similarly, the mediolateral segregation of premotor interneurons innervating flexor and extensor motor neurons is linked to their pattern of sensory input (Tripodi et al., 2011). Nevertheless, cell recognition molecules, individually or combinatorially, have long been argued to underlie specificity in synaptic connectivity (Sanes and Yamagata, 2009; Shen and Scheiffele, 2010; Williams et al., 2010). Yet, in most regions of the mammalian CNS, genetic support for the operation of molecular programs that determine target specificity remains elusive.

One neural system in which the cellular origins of synaptic specificity have been examined in some detail is the spinal monosynaptic stretch reflex circuit. Here, the fine pattern of sensory-motor connectivity has been defined through a combination of anatomical and physiological studies (Brown, 1981; Ladle et al., 2007). In this circuit, group Ia proprioceptive afferent fibers make strong connections with motor neurons supplying the same muscle and weaker connections with motor neurons supplying synergistic muscles (Eccles et al., 1957; Frank and Mendelson, 1990). Afferent connections are rarely if ever formed with motor neurons supplying functionally unrelated or antagonistic muscles (Eccles et al., 1957; Frank and Mendelson, 1990).

Do recognition molecules establish selective sensory-motor connections in this circuit? Classical cadherins, a major class of calcium-dependent cell adhesion molecules, are expressed by functionally matched subsets of proprioceptive sensory and motor neurons (Price et al., 2002) and have been implicated in regulating synaptic specificity in other regions of the CNS, but not yet in spinal cord (Clandinin and Feldheim, 2009; Osterhout et al., 2011; Williams et al., 2011). A second class of recognition molecules, semaphorins and their plexin and neuropilin receptors, are expressed by subsets of sensory and motor neurons (Cohen et al., 2005). Indeed, the motor pool-selective expression of semaphorin3E (Sema3E) has been shown to gate one specialized aspect of sensory-motor connectivity—the basic decision of whether to form a direct connection or to influence motor output only indirectly (Pecho-Vrieseling et al., 2009). At brachial levels of the spinal cord, cutaneus maximus (Cm) motor neurons differ from other motor pools in that they lack direct

proprioceptive sensory input (Vrieseling and Arber, 2006). This unusual pattern of connectivity appears to have its basis in the Sema3E-mediated exclusion of direct sensory-motor connections, through engagement of a sensory receptor, PlexinD1 (Pecho-Vrieseling et al., 2009). Thus, within this sensory-motor reflex arc, the status of Sema3E-PlexinD1 signaling determines whether motor neurons receive direct proprioceptive sensory input. Whether the mechanisms that govern the exclusion of sensory input have any bearing on those that determine the fine-grained pool-by-pool patterns of monosynaptic sensory-motor input remains unclear. In principle, precise fine-grained sensory-motor specificity could emerge through an entirely different process of target recognition or even through the action of motor neuron-independent targeting signals.

We have used molecular genetic manipulations to examine whether Sema3E-PlexinD1 signaling is a determinant of the fine pattern of monosynaptic sensory-motor connections at lumbar levels of the mouse spinal cord. We find that Sema3E is expressed by motor neurons that supply the gluteus (Glu), a hip extensor muscle, but not by motor neurons innervating the hamstring (Ham) knee flexor muscle. Conversely, *PlexinD1* is expressed by many Ham proprioceptors but by few Glu proprioceptors. Electrophysiological and anatomical analysis reveals that ectopic expression of Sema3E in Ham motor neurons markedly reduces the incidence of homonymous inputs from Ham sensory afferents. Conversely, attenuation of Sema3E-PlexinD1 signaling through genetic inactivation of ligand or receptor results in an altered pattern of monosynaptic connectivity, such that Ham proprioceptive afferents now innervate Glu motor neurons. These findings provide genetic evidence that Sema3E-PlexinD1 repellent signaling helps to determine the fine-grained pattern of sensory-motor connections in mammalian monosynaptic sensory reflex arcs. More generally, our findings indicate that sensory recognition of target motor neurons has a role in establishing the precise pattern of sensory-motor connections in mammalian spinal cord.

RESULTS

Sema3E and *PlexinD1* Expression Defines Subsets of Motor Neurons and Sensory Neurons

To determine whether lumbar motor neuron pools express Sema3E, we injected rhodamine-conjugated dextran (Rho-Dex) into different hindlimb muscle groups. We targeted the Glu, biceps femoris—a Ham muscle, rectus femoris (Rf), and adductor (Ad) muscles. Injections were performed in embryonic day 14.5 (E14.5)–E15.5 *Sema3E-nlsLacZ* embryos in which nuclear LacZ is expressed faithfully from one *Sema3E* allele (Pecho-Vrieseling et al., 2009). We found that in *Sema3E-nlsLacZ* heterozygous embryos, LacZ was expressed by all Glu motor neurons (Figures 1A–1D), but not by more dorsally positioned Ham, Rf, or Ad motor neurons (Figures 1A–1D; data not shown).

We next determined the profile of *PlexinD1* expression in DRG neurons at lumbar levels two to five in E17.5 embryos. In wild-type mice, we detected high-level expression of *PlexinD1* in DRG neurons (Figure S1A) and found that expression was almost completely absent from lumbar DRG in *trkC* mutants (Figure S1B), which are depleted of proprioceptive sensory neurons (Klein et al., 1994). Thus, in lumbar, as in brachial DRG (Pecho-Vrieseling et al., 2009), *PlexinD1* expression is enriched in proprioceptive sensory neurons. To resolve the profile of *PlexinD1* expression by specific classes of DRG neurons, we compared the expression of *PlexinD1* with that of *parvalbumin* (*Pv*), a marker of proprioceptive sensory neurons (Arber et al., 2000; Honda, 1995). Strong expression of *PlexinD1* was detected in ~70% of Pv^+ proprioceptive sensory neurons (Figures S1C–S1E). Binding of alkaline phosphatase (AP)-Sema3E was not detected in *PlexinD1* mutant spinal cord (see Chauvet et al., 2007; Gu et al., 2005) (Figures S1I–S1L). Moreover, strong expression of *PlexinD1* was absent from $Npn1^+$ DRG neurons (Figures S1F–S1H), arguing that PlexinD1 is a relevant receptor for Sema3E in the developing lumbar spinal cord.

We then analyzed the status of *PlexinD1* expression in DRG neurons that supply Glu and Ham muscles. We found that ~40% of Glu proprioceptive sensory neurons (Rho-Dex^+ and Pv^+) expressed *PlexinD1* (Figures 1E–1H), whereas ~70% of Ham proprioceptive sensory neurons expressed *PlexinD1* (Figures 1I–1M). The expression of *PlexinD1* by only a subset of proprioceptors is reminiscent of findings in cervical level DRG (Pecho-Vrieseling et al., 2009), where ~80% of Cm and ~50% of triceps (Tri) proprioceptors express *PlexinD1*.

Monosynaptic Connectivity in Ham and Glu Sensory Reflex Arcs

Our functional analysis of Sema3E-PlexinD1 signaling focused on $Sema3E^+$ Glu and $Sema3E^{off}$ Ham sensory-motor reflex arcs because these two motor neuron subtypes innervate muscles that control different leg joints, and occupy overlapping rostrocaudal levels of the lumbar spinal cord (Sürmeli et al., 2011) (Figures 1A–1D; data not shown). In *Sema3E-nlsLacZ* heterozygous and homozygous mice analyzed at postnatal day 1 (P1), we detected no obvious difference in the positioning of $Sema3E^{on}$ motor neurons at caudal lumbar levels, evaluated by X-gal staining (Figures S2A and S2B). In addition, the degree of arborization of Glu motor neuron dendrites, visualized by Rho-Dex injection into the Glu muscle at P10, was similar in *Sema3E-nlsLacZ* homozygous and heterozygous mice (Figures S2C and S2D).

We performed intracellular recording from identified motor neurons in isolated P5–P7 spinal cord preparations to determine the wild-type status of Ham and Glu connectivity in sensory-motor reflex arcs (Figure 2A). The presence of monosynaptic inputs in response to stimulation of Ham or Glu sensory afferents was assessed by monitoring the onset latency and jitter of sensory-evoked excitatory postsynaptic potentials (EPSPs) (Vrieseling and Arber, 2006; Doyle and Andresen, 2001; Rose and Metherate, 2005). Short latency inputs with a variance in onset latency of <0.2 following repeated trials were designated as monosynaptic in origin (Vrieseling and Arber, 2006; Doyle and Andresen, 2001; Rose and Metherate, 2005). Using this criterion, we determined the status of homonymous (Ham sensory-evoked responses in Ham motor neurons and Glu sensory-evoked responses in Glu motor neurons) connections in wild-type mice and nonrecombined $PlexinD1^{flox/flox}$ controls. The mean onset latency of Ham homonymous monosynaptic connections was 6.5 ± 0.5 ms (mean latency ± SEM; seven neurons, n = 6 mice) with a mean EPSP amplitude of 5.3 ± 0.8 mV (Figures 2B, 2F,

Cell PRESS
Open ACCESS

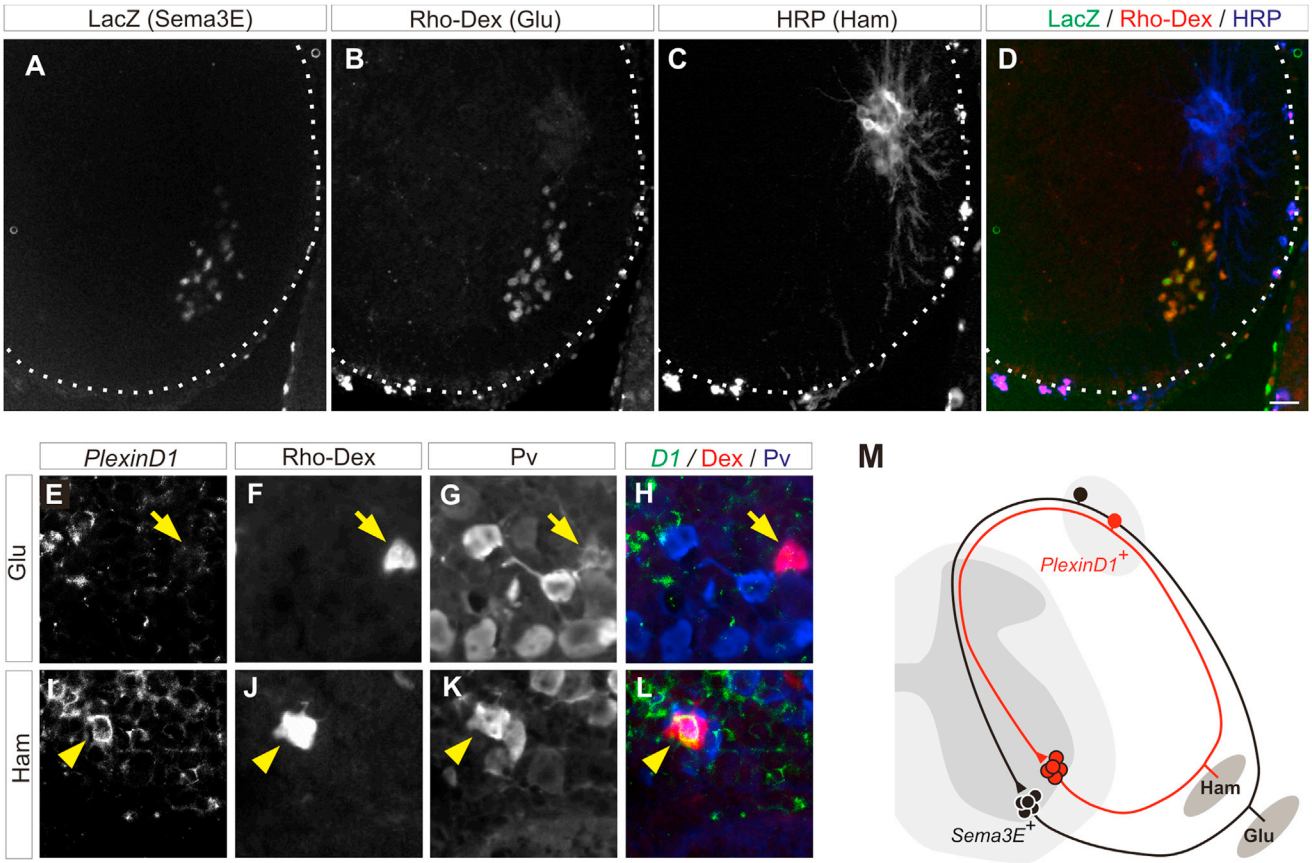

Figure 1. Absence of Matching *Sema3E-PlexinD1* Expression in Glu and Ham Motor and Sensory Neurons

(A–D) Sema3E^{+} motor neurons were detected by LacZ (A) after retrograde Rho-Dex tracing from Glu (B) and HRP tracing from Ham (C) muscles of E14.5 *Sema3E*$^{nlz/+}$ embryos. (D) is merge. The scale bar represents 25 μm (D).

(E–L) *PlexinD1* expression in Pv^{+} proprioceptive sensory neurons after Rho-Dex tracing from Glu (E–H) and Ham (I–L) muscles of E14.5 embryos is presented. Arrows indicate Pv^{+}, Rho-Dex^{+}, and *PlexinD1*^{off} proprioceptive sensory neurons. Arrowheads indicate Pv^{+}, Rho-Dex^{+}, and *PlexinD1*$^{+}$ proprioceptive sensory neurons.

(M) Diagram shows the summary of the expression of *Sema3E* and *PlexinD1*.

See also Figure S1.

2G, and S3A). Glu monosynaptic homonymous connections had a mean onset latency of 6.4 ± 0.4 ms (nine neurons, n = 7 mice) and a mean EPSP amplitude of 3.9 ± 0.6 mV (Figures 2C, 2F, 2G, and S3B).

We next probed the existence of heteronymous (Ham sensory-Glu motor neuron or Glu sensory-Ham motor neuron) monosynaptic connectivity. We compared the mean onset latency of heteronymous responses with a mean onset latency of homonymous responses determined as monosynaptic by jitter analysis. A low-amplitude EPSP of 0.8 ± 0.2 mV with a mean onset latency of 5.7 ± 0.4 ms (nine neurons, n = 7 mice) was observed in Glu motor neurons after Ham sensory stimulation (Figures 2D, 2F, 2G, and S3C). In contrast, stimulation of Glu sensory nerves while recording from Ham motor neurons did not elicit monosynaptic EPSPs (seven neurons, n = 7 mice; Figures 2E, 2F, and 2G). These results indicate that there are, at best, only sparse monosynaptic connections between heteronymous sensory-motor pairs projecting to these two functionally unrelated muscles.

Ectopic Expression of Sema3E in Motor Neurons Suppresses Homonymous Sensory-Motor Connections

The expression of Sema3E by Glu but not Ham motor neurons led us to explore whether the absence of *Sema3E* expression by Ham motor neurons is required for the formation of monosynaptic connections between Ham sensory and motor neurons and, conversely, whether expression of *Sema3E* by Glu motor neurons and *PlexinD1* by Ham sensory neurons prevents inappropriate monosynaptic connections between Ham sensory afferents and Glu motor neurons.

To express Sema3E ectopically in limb-innervating motor neurons, we generated a mouse line in which a floxed *Sema3E* cassette was introduced into the *Tau* gene locus (*lsl-Sema3E-iresGFP* mice) (Figure 3A). We crossed *lsl-Sema3E-iresGFP* mice with *Olig2-Cre* line in which Cre is expressed by motor neuron progenitors (Sürmeli et al., 2011, Dessaud et al., 2007). In situ hybridization analysis showed that *Sema3E* expression in motor neurons of E15.5 *lsl-Sema3E-iresGFP* embryos was 13.7 ± 1.3-fold higher than that of wild-type mice (Figure S4).

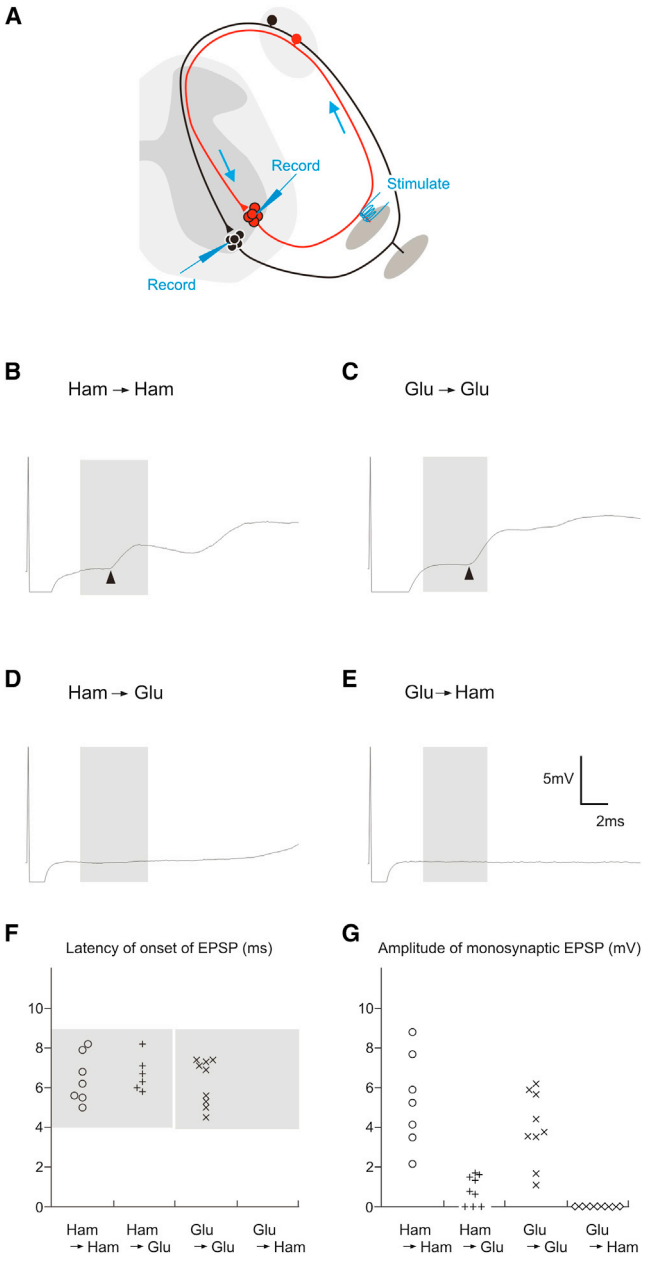

Figure 2. Analysis of Ham and Glu Monosynaptic Sensory-Motor Circuitry by Electrophysiology

(A) Diagram shows intracellular recording from motor neurons upon muscle nerve stimulation.

(B–E) Individual EPSP traces of intracellular recordings from Ham motor neurons upon Ham (B) or Glu (E) muscle nerve stimulation, and from Glu motor neurons upon Glu (C) or Ham (D) muscle nerve stimulation, are presented. All traces were recorded at 1 Hz and averaged 20 times. Arrowheads indicate onset latency of the monosynaptic EPSPs. Gray bins show the range of monosynaptic latency windows.

(F) Quantification of the latency of the onset of EPSPs is shown. Gray bins show the range of monosynaptic latency windows: 4.0–8.9 ms for Ham-Ham, and 3.8–8.9 ms for Glu-Glu. The monosynaptic window is defined as the mean ± 2 SD of monosynaptic latency of wild-types.

(G) Quantification of amplitude of monosynaptic EPSPs is presented.

See also Figure S3.

In P0 *Olig2-Cre; lsl-Sema3E-iresGFP* mice, both Sema3E and GFP were expressed in most lumbar motor neurons (Figures 3E–3G and 3L–3O). In the spinal cord of *Olig2-Cre; lsl-Sema3E-iresGFP* mice, Pv^+ proprioceptive sensory axons reached the ventral spinal cord and showed an axonal projection pattern similar to that in wild-type mice (Figures 3B–3O). Thus, ectopic expression of Sema3E does not obviously perturb the trajectory of proprioceptive sensory axons as they project into the ventral spinal cord.

To determine whether loss of Sema3E expression from Ham motor neurons is required for the wiring specificity of monosynaptic sensory-motor connections, we recorded intracellularly from Ham motor neurons and stimulated Ham sensory nerves (Figure 4A). In *Olig2-Cre; lsl-Sema3E-iresGFP* mice (14 neurons, n = 5 mice), the mean amplitude of the monosynaptic EPSP was 1.9 ± 0.6 mV (Figures 4B–4E), a 2.8-fold reduction from wild-type ($p < 0.05$). Individually, 5 out of 14 Ham motor neurons in *Olig2-Cre; lsl-Sema3E-iresGFP* mice lacked detectable monosynaptic input from Ham sensory neurons (Figures 4B–4E). Thus, ectopic expression of Sema3E in Ham motor neurons reduces the incidence of monosynaptic sensory-motor connections from Ham sensory neurons.

We considered whether the reduction in strength of monosynaptic sensory-motor connections in *Olig2-Cre; lsl-Sema3E-iresGFP* mice might reflect a decrease in the efficacy of transmission at individual synapses, rather than a loss of connections. To address this issue, we examined whether acute application of recombinant Sema3E to isolated spinal cord could regulate the synaptic transmission at presynaptic sites. Exposure to Sema3E recombinant protein (5 nM) did not alter the mean amplitude of the monosynaptic sensory-evoked component of the compound response of motor axons contributing to L5 ventral root compared to exposure to control Fc protein (ratio of 1.05 ± 0.15 at 30 min and 0.99 ± 0.31 at 90 min; n = 3 mice). Thus, acute exposure to Sema3E appears not to inhibit transmission at sensory-motor synapses.

We therefore determined the density of sensory synaptic contacts on control and Sema3E-expressing Ham motor neurons. Rho-Dex was injected into the Ham muscle in P5 wild-type and *Olig2-Cre*; *lsl-Sema3E-iresGFP* mice, and we analyzed the density of vesicular glutamate transporter 1 (vGlut1)—marked proprioceptive synapses 48 hr later (Alvarez et al., 2004; Betley et al., 2009). We detected a 53% decrease in the number of $vGlut1^+$ boutons on the soma of Rho-Dex^+ Ham motor neurons in *Olig2-Cre*; *lsl-Sema3E-iresGFP* mice compared to wild-type controls (wild-type, 39.6 ± 5.7, n = 12 neurons from five mice; *Olig2-Cre*; *lsl-Sema3E-iresGFP*, 20.92 ± 5.15, n = 12 neurons from four mice; $p < 0.05$; Figures 5C, 5D, and 5E). In contrast, the density of vGlut1 boutons in the vicinity of, but not in contact with, Ham motor neuron somata was similar in wild-type and *Olig2-Cre*; *lsl-Sema3E-iresGFP* mice (Figures 5A and 5B). Thus, the presynaptic terminals of proprioceptive sensory axons in *Olig2-Cre*; *lsl-Sema3E-iresGFP* mice arrive in the vicinity of Ham motor neurons but make relatively few direct contacts.

We also examined whether elevating further, the level of expression of Sema3E in $Sema3E^+$ Glu motor neurons changes the density of sensory synaptic contacts. To assess this, we injected Rho-Dex into the Glu muscle in wild-type and *Olig2-Cre*;

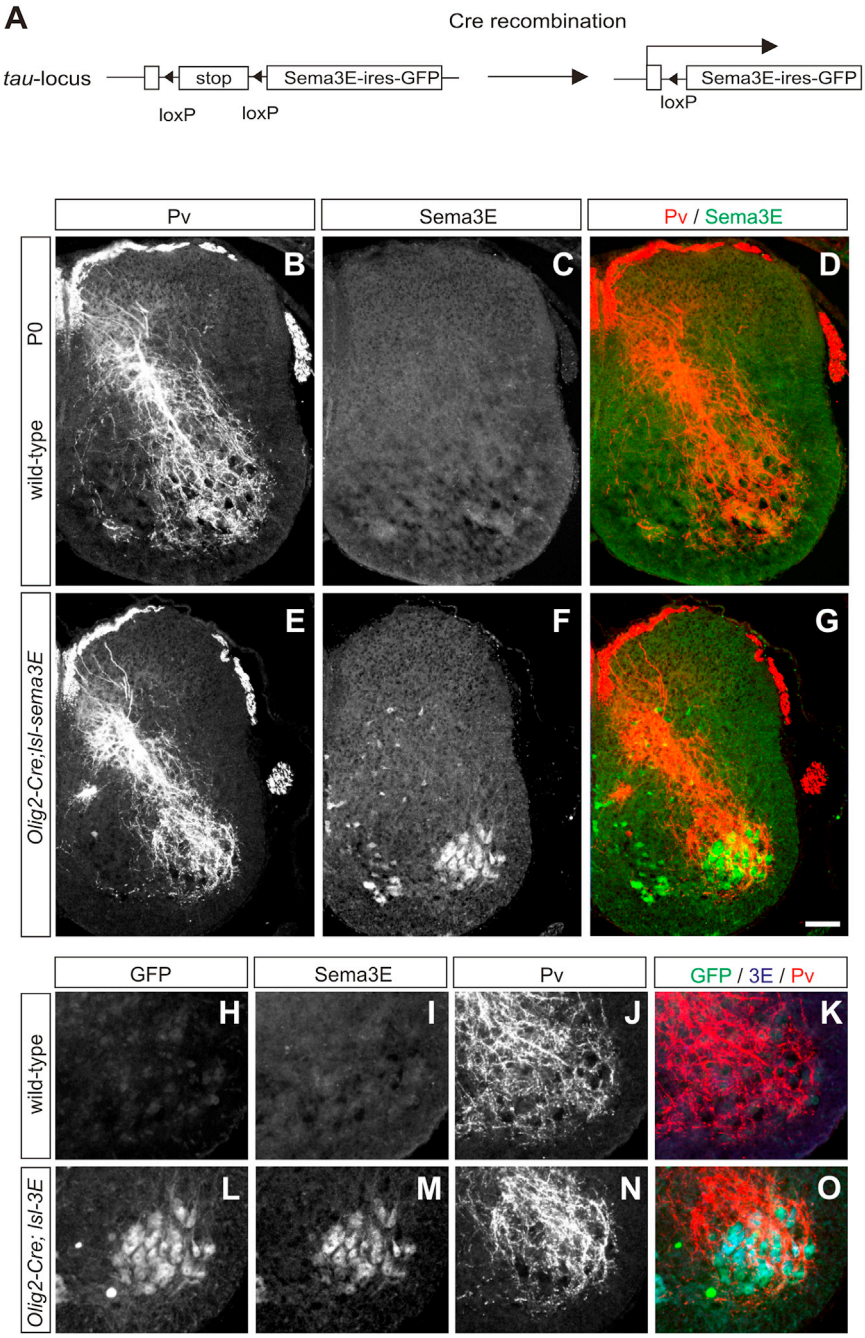

Figure 3. Ectopic Expression of Sema3E by Motor Neurons Does Not Affect Proprioceptive Sensory Axon Trajectory

(A) Schematic diagram shows the strategy of ectopic expression of Sema3E in motor neurons. In the absence of Cre recombinase, a transcriptional stop sequence flanked by loxP sites inhibits expression of *Sema3E* from its start codon. The integrated targeting cassette allows for conditional expression of Sema3E and GFP upon Cre recombinase-mediated activation.

(B–G) Analysis of Pv^{+} sensory axons in the spinal cord in P0 wild-type (B–D) and *Olig2-Cre; lsl-sema3-iresGFP* (E–G) mice is shown. The scale bar represents 50 μm (G).

(H–O) Higher magnification of the images of the ventral spinal cord in wild-type (H–K) and *Olig2-Cre; lsl-Sema3E-iresGFP* (L–O) mice is presented. See also Figure S4.

Loss of *Sema3E* or *PlexinD1* Alters the Specificity of Sensory-Motor Connections

To examine whether Sema3E-PlexinD1 signaling controls the fine specificity of monosynaptic sensory-motor connections, we analyzed *Sema3E* null mutant and $PlexinD1^{flox/-}$; *Wnt1-Cre* mice (Figures S5A and S5B) (Pecho-Vrieseling et al., 2009; Danielian et al., 1998; Zhang et al., 2009). Although Cre is expressed in both the DRG and dorsal spinal cord of *Wnt1-Cre* mice (Danielian et al., 1998; Zhang et al., 2009), Cre expression in the dorsal spinal cord is unlikely to result in sensory-motor connectivity or dorsal-patterning defects because *PlexinD1* is not expressed by spinal cord neurons.

We first determined the status of homonymous monosynaptic connections of Ham and Glu sensory-motor circuits in *Sema3E* mutants and $PlexinD1^{flox/-}$; *Wnt1-Cre* mice. The homonymous monosynaptic EPSP latency measured in Ham motor neurons was 5.9 ± 0.2 ms with an EPSP amplitude of 3.8 ± 0.6 mV in *Sema3E* mutants (seven neurons, n = 7 mice; Figures S5C and S5E), and in $PlexinD1^{flox/-}$; *Wnt1-Cre* mice, 6.4 ± 0.2 ms with an EPSP amplitude of 5.2 ± 0.6 mV (22 neurons, n = 13 mice; Figures S5C and S5E). In *Sema3E* mutants, monosynaptic inputs from Glu afferents to Glu motor neurons exhibited a mean onset latency of 6.8 ± 0.4 ms with an EPSP amplitude of 4.6 ± 1.0 mV (eight neurons, n = 8 mice; Figures S5D and S5F). Similarly, in $PlexinD1^{flox/-}$; *Wnt1-Cre* mice, monosynaptic latencies were 6.5 ± 0.3 ms with an EPSP amplitude of 3.2 ± 0.7 mV (11 neurons, n = 11 mice; Figures S5D and S5F). The mean onset latency and EPSP amplitude values for Ham and Glu monosynaptic

lsl-Sema3E-iresGFP mice. We did not find a significant difference in $vGlut1^{+}$ boutons on $Rho\text{-}Dex^{+}$ Glu motor neurons between wild-type and *Olig2-Cre*; *lsl-Sema3E-iresGFP* mice (wild-type, 16.8 ± 2.0, n = 19 neurons from four mice; *Olig2-Cre*; *lsl-Sema3E-iresGFP*, 14.4 ± 2.2, n = 20 neurons from three mice). This finding indicates that a further elevation in Sema3E expression levels in motor neurons, superimposed on endogenous Sema3E expression, does not repel sensory inputs, arguing for a view that Sema3E functions in an absolute, rather than graded, manner to define sensory-motor connection patterns.

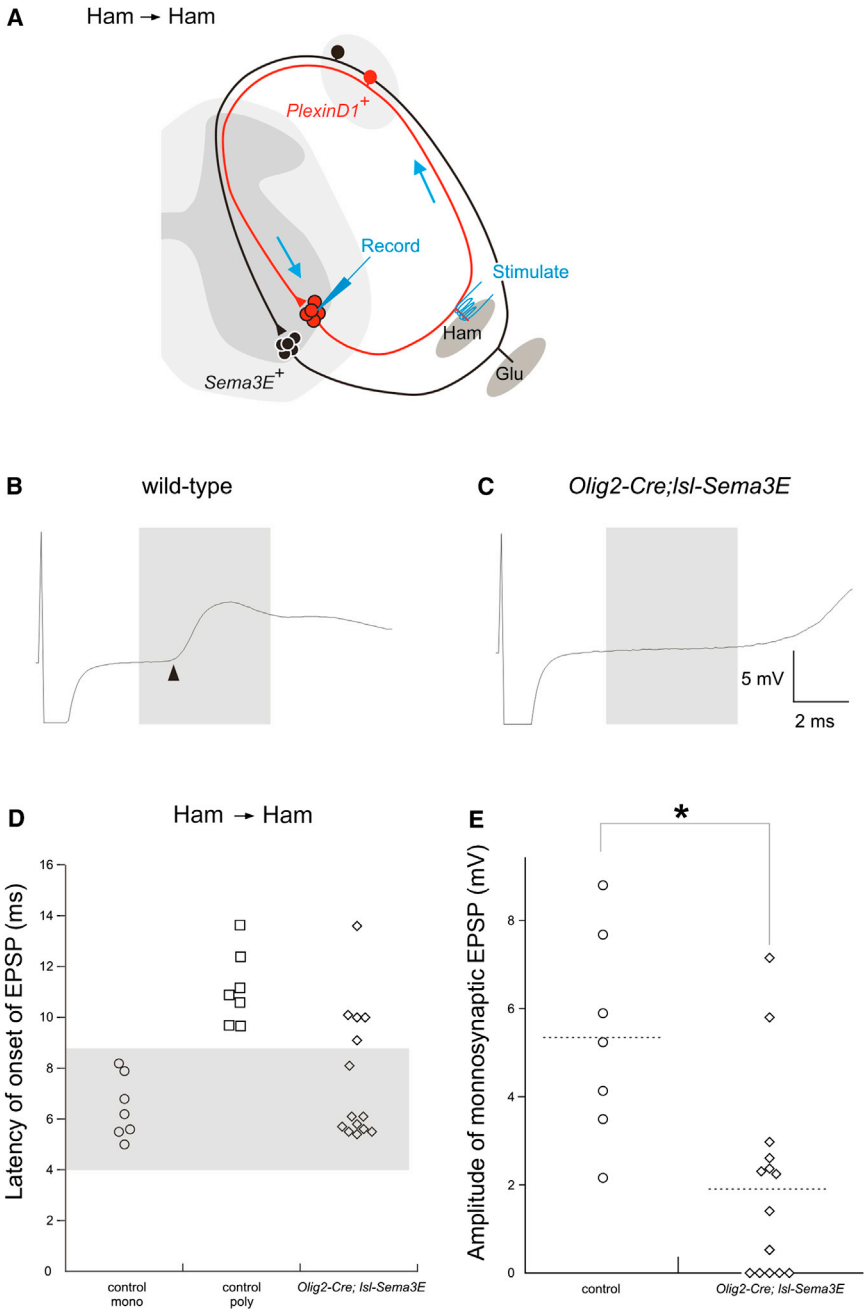

Figure 4. Ectopic Expression of Sema3E by Motor Neurons Suppresses Monosynaptic Sensory-Motor Connectivity

(A) Diagram presents intracellular recording from Ham motor neurons upon Ham muscle nerve stimulation.

(B and C) Individual EPSP traces of intracellular recordings from Ham motor neurons of wild-type (B) and *Olig2-Cre; lsl-Sema3E-iresGFP* (C) mice upon Ham muscle nerve stimulation are shown. All traces were recorded at 1 Hz and averaged 20 times. Gray bins indicate the monosynaptic latency windows, and arrowheads indicate onset latency of the monosynaptic EPSPs. The trace from some *Olig2-Cre; lsl-Sema3E-iresGFP* mice did not show homonymous monosynaptic EPSPs (C).

(D) Quantification of the latency of the onset of EPSPs from individual Ham motor neurons upon Ham muscle nerve stimulation is shown. Gray bin indicates monosynaptic latency windows. The plots for controls are the same as in Figure 2F.

(E) Quantification of the amplitude of the monosynaptic EPSPs is presented. The 0 mV indicates no monosynaptic EPSPs. Of 14 Ham motor neurons from *Olig2-Cre; lsl-Sema3E-iresGFP* mice, 5 did not show homonymous monosynaptic EPSPs. Horizontal lines indicate the mean amplitude. There are significant differences between control and *Olig2-Cre; lsl-Sema3E-iresGFP* mice (*$p < 0.05$, paired t test).

See also Figure S2.

connections in *Sema3E* mutants and in *PlexinD1*$^{flox/-}$*; Wnt1-Cre* mice were similar to wild-type mice and littermate controls (Figures 2F, 2G, S5C–S5F, and S5I). Thus, the loss of *Sema3E* or *PlexinD1* does not actively alter the pattern of Ham and Glu homonymous monosynaptic sensory-motor connections.

We next investigated the status of ectopic sensory-motor connections, analyzing first the presence of Ham sensory input to Glu motor neurons (Figures 6A, S5G, and S5H). In contrast to wild-type mice and littermate controls, we found that 44% of Glu motor neurons (4 out of 9 neurons, n = 9 mice) in *Sema3E* mutant and 45% of Glu motor neurons (5 out of 11 neurons, n = 11 mice) in *PlexinD1*$^{flox/-}$*; Wnt1-Cre* mice exhibited a large amplitude of monosynaptic EPSP (*Sema3E* mutants, 3.0 ± 0.7 mV; *PlexinD1*$^{flox/-}$*; Wnt1-Cre* mice, 5.3 ± 1.6 mV) (Figures 6B–6G). Thus, Ham proprioceptive axons form functional monosynaptic connections with Glu motor neurons in both *Sema3E* mutant and *PlexinD1*$^{flox/-}$*; Wnt1-Cre* mice. In contrast, we failed to detect inappropriate input from Glu sensory afferents to Ham motor neurons in *Sema3E* mutant (13 neurons, n = 8 mice) or *PlexinD1*$^{flox/-}$*; Wnt1-Cre* mice (13 neurons, n = 10 mice) (Figures S5I and S5J). Thus, defects in monosynaptic sensory-motor specificity in *Sema3E* mutant and *PlexinD1*$^{flox/-}$*; Wnt1-Cre* mice are restricted to *PlexinD1*^{on} Ham Ia sensory afferents and *Sema3E*^{on} Glu motor neurons.

DISCUSSION

The selectivity of reflex connections formed by proprioceptive sensory and motor neurons obeys two empirical rules: only certain subclasses of proprioceptors form direct connections with spinal motor neurons, and those that do form connections, select their postsynaptic targets with exquisite functional

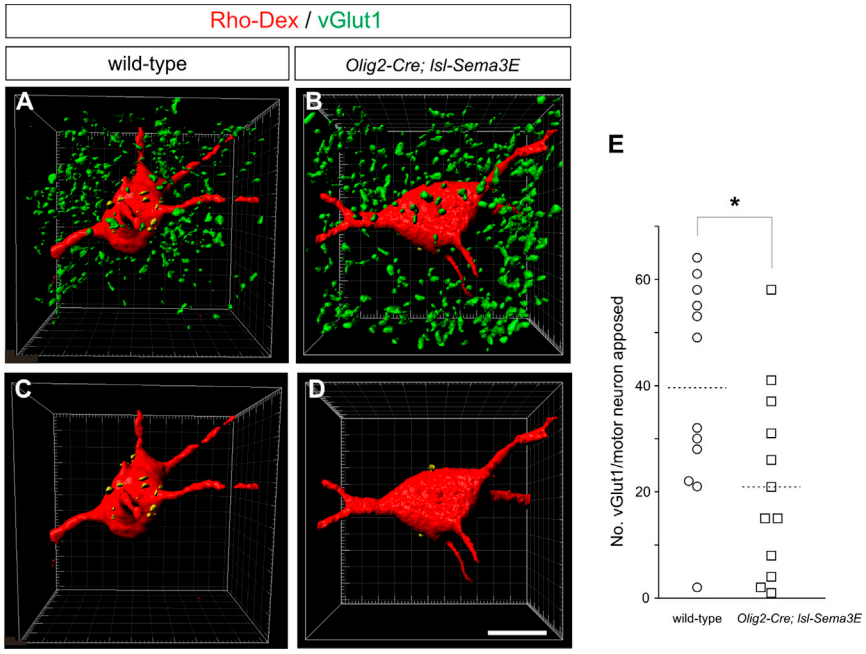

Figure 5. Ectopic Expression of Sema3E in Motor Neurons Reduces Contacts between Proprioceptive Sensory Terminals and Motor Neurons

(A–D) Analysis of vGlut1 apposition with Rho-Dex-labeled Ham motor neurons by Imaris is shown. The yellow or green dots indicate contact or noncontact sites, respectively (A–D). (C) and (D) show only yellow sites on motor neurons from (A) and (B). The scale bar represents 15 μm (D).

(E) The quantification of numbers of vGlut1 apposition on the Rho-Dex$^+$ Ham motor neurons is shown. There are significant differences between control and *Olig2-Cre; Isl-Sema3E-iresGFP* mice (*$p < 0.05$, paired t test).

specificity. The mechanisms that direct selective patterns of monosynaptic sensory-motor connections have yet to be defined. Our genetic findings show that Sema3E-PlexinD1 signaling helps to sculpt the selectivity of monosynaptic sensory-motor connections by suppressing the formation of inappropriate sensory connections with functionally unrelated motor neuron pools.

Prior studies at brachial levels of the spinal cord have provided evidence that Sema3E-PlexinD1 repellent signaling underlies the normal failure of certain classes of proprioceptive sensory afferents to form direct connections with their cognate motor neuron pools (Pecho-Vrieseling et al., 2009). But appreciation of the role of Sema3E signaling as an arbiter of direct or indirect connectivity does not resolve the issue of whether sema-plexin signaling has an additional role in defining the fine connection specificity exhibited in more typical monosynaptic sensory-motor reflex arcs. Our analysis of sensory-motor connectivity patterns at lumbar levels of the spinal cord, both after ectopic motor neuron expression of Sema3E and, more persuasively, through genetic elimination of Sema3E and its cognate sensory receptor PlexinD1, reveals that the restriction of homonymous monosynaptic connections in the Ham sensory reflex arc is achieved, in part, by the pool-by-pool selectivity in expression of Sema3E: most notably on Glu but not Ham motor neurons (Figure 7).

Together, our findings provide insight into the role of repellent Sema3E signaling in sensory-motor connectivity. In particular, they establish one molecular mechanism for determining the fine pool specificity of direct monosynaptic connections. Viewed from the perspective of the target selectivity of Ham proprioceptive afferents for Glu or Ham motor neurons, our results indicate a causal role for pool-restricted motor neuron Sema3E expression in directing a binary target choice (Figure 7). In few other instances have gain- and loss-of-function studies on genes encoding molecular target recognition been shown to determine a binary choice in synaptic connectivity in the mammalian CNS. Perhaps the most relevant precedent concerns the function of selective wnt-mediated repellent signaling in gating the binary innervation specificity of two potential target muscle groups in *Drosophila* (Inaki et al., 2007).

Our findings also emphasize several unresolved issues about the role of Sema3E-PlexinD1 repellent signaling as a determinant of the fine specificity of sensory-motor connections. Analysis of the profile of *PlexinD1* expression by proprioceptive sensory neurons in the Ham and Glu reflex arcs, together with the related studies of Pecho-Vrieseling et al. (2009) in the Cm and Tri reflex arcs, indicates that *PlexinD1* expression profiles are more complex than predicted by a simple binary view of connection selectivity. Some 40% of Glu proprioceptive sensory afferents express *PlexinD1*, at face value precluding them from connecting with Glu motor neurons. Moreover, only about 70% of Ham sensory neurons express *PlexinD1*, raising the question of why the remaining 30% of sensory afferents fail to form connections with Glu motor neurons. One possible explanation is that those proprioceptive sensory neurons that lack *PlexinD1* correspond to group Ib afferents, which normally lack direct connections with motor neurons.

Our findings suggest that molecular recognition of motor neuron targets operates in parallel with a motor neuron-independent dorsoventral tier-targeting system (Sürmeli et al., 2011) to establish the specificity of connections in sensory-motor reflex arcs. We note that Glu and Ham motor neurons occupy adjacent dorsoventral tiers (Sürmeli et al., 2011) (Figures 1A–1D), and thus, for motor neurons at the border of these two pools, tier-targeting mechanisms are unlikely to have sufficient precision to exclude cross-connectivity. Motor neuron-based recognition systems may therefore be needed to consolidate and reinforce initial tier-based restrictions in connectivity. In addition, it is notable that the erosion of sensory-motor specificity in the Glu and Ham reflex arcs is unidirectional: in *Sema3E* and *PlexinD1* mutant mice, Ham sensory afferents synapse with Glu motor neurons, whereas Glu sensory afferents fail to contact Ham motor neurons. Thus, the Sema3E-PlexinD1 recognition system may operate only within a narrowly circumscribed set of reflex

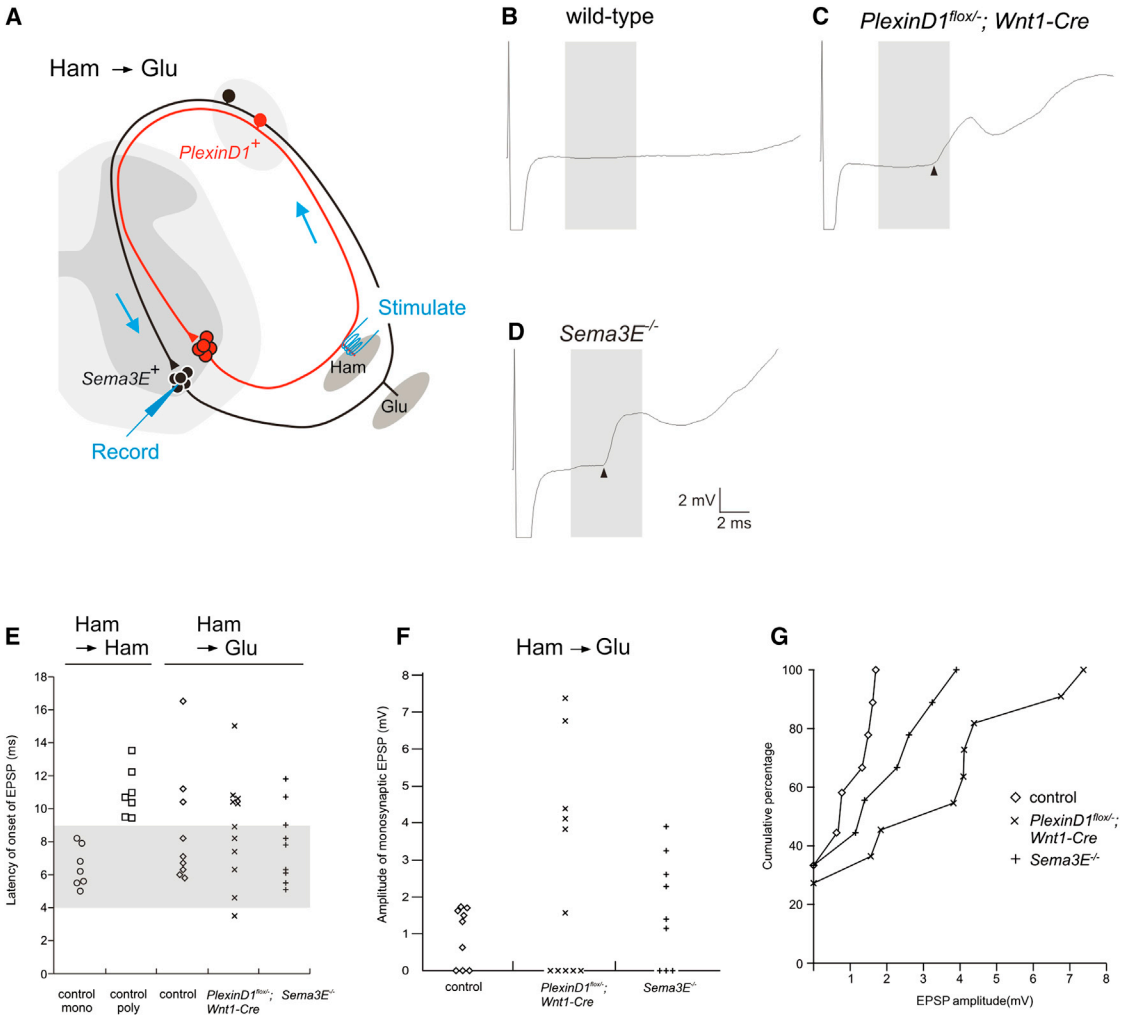

Figure 6. Loss of Sema3E or PlexinD1 Function Disturbs Specificity of Monosynaptic Sensory-Motor Connections

(A) Diagram shows intracellular recording from Glu motor neurons upon Ham muscle nerve stimulation.

(B–D) Individual EPSP traces of intracellular recordings from Glu motor neurons of wild-type (B), *PlexinD1*$^{flox/-}$*; Wnt1-Cre* (C), and *Sema3E*$^{-/-}$ mice (D) upon Ham muscle nerve stimulation are presented. All traces were recorded at 1 Hz and averaged 20 times. Gray bins indicate the monosynaptic latency window, and arrowheads indicate the onset latency of monosynaptic EPSPs.

(E) Quantification of the latency of the onset of EPSPs is shown. The left two columns are from individual Ham motor neurons upon Ham nerve stimulation in control mice, and the right three columns are from individual Glu motor neurons upon Ham muscle nerve stimulation in control, *PlexinD1*$^{flox/-}$*; Wnt1-Cre*, and *Sema3E*$^{-/-}$ mice. Gray bin indicates the monosynaptic latency windows.

(F) Quantification of amplitude of monosynaptic EPSPs in Glu motor neurons upon Ham muscle nerve stimulation is shown. The 0 mV indicates no monosynaptic EPSPs. A total of 45% (5 out of 11) of *PlexinD1*$^{flox/-}$*; Wnt1-Cre* mice and 44% (four out of nine) of *Sema3E* mutant mice showed more than 2 mV of the monosynaptic EPSPs.

(G) The cumulative frequency histograms of (F) are presented.

See also Figure S5.

arcs, implying the existence of Sema3E-independent systems for sensory-motor specificity.

The nature of inferred Sema3E-independent recognition systems for sensory-motor specificity remains unclear. Other semaphorins are expressed by subsets of spinal motor neurons (Cohen et al., 2005), and thus, a more general system of semaphorin coding could constitute a pervasive recognition strategy for spinal sensory-motor connectivity, with different sema subgroups functioning in distinct reflex arcs. Sema-independent recognition systems could also contribute to sensory-motor specificity, with known expression profiles suggesting the possible involvement of eph-ephrin repellent, and cadherin-adhesive systems (Price et al., 2002; Iwamasa et al., 1999). Despite these uncertainties, our genetic analysis of connectivity in Glu and Ham reflex arcs provides rare gain- and loss-of-function evidence that repellent signaling determines binary target recognition and fine synaptic specificity in the mammalian CNS.

Finally, we note that Sema3E-PlexinD1 signaling has also been implicated in the pattern of connectivity in thalamostriatal circuits. Intriguingly, a distinct logic of *Sema3E* and *PlexinD1*

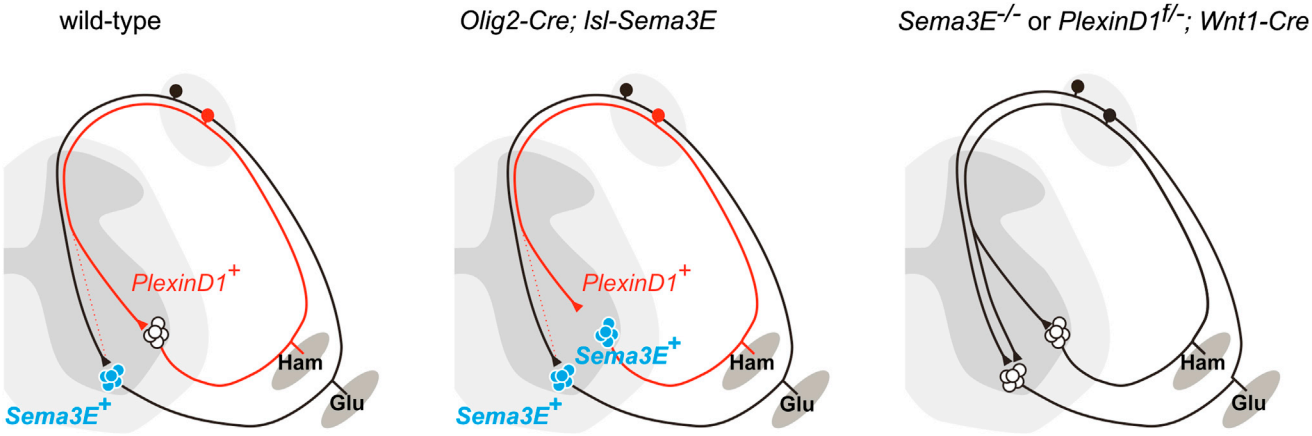

Figure 7. Roles of Sema3E-PlexinD1 Signaling at Lumbar Levels of the Spinal Cord

At lumbar levels of the spinal cord, Sema3E-PlexinD1 signaling suppresses inappropriate synaptic connections between Ham sensory afferents and Glu motor neurons. Ectopic expression of Sema3E in Ham motor neurons prevents the strength of homonymous sensory-motor connections between Ham sensory afferents and Ham motor neurons. Moreover, in the absence of Sema3E-PlexinD1 signaling, there were aberrant strong monosynaptic connections between Ham sensory afferents and Glu motor neurons.

expression in pre- and postsynaptic neurons appears to operate here: *Sema3E* is expressed by presynaptic neurons in the thalamus and *PlexinD1* by postsynaptic neurons in the striatum (Ding et al., 2012). In this region of the mammalian CNS, Sema3E-PlexinD1 signaling may regulate thalamostriatal synapses indirectly, through the gating or induction of other recognition systems. The existence of diverse modes of Sema3E-PlexinD1 signaling could serve to augment the recognition functions available to this dedicated ligand-receptor pair.

EXPERIMENTAL PROCEDURES

All animals were treated according to institutional and National Institutes of Health guidelines approved by the Institutional Animal Care and Use Committee at Cincinnati Children's Hospital Medical Center.

Generation of *Isl-Sema3E-iresGFP* Mice

A lox-stop-lox-Sema3E-ires-GFP-polyA-targeting cassette was integrated into exon 2 of the *Tau* locus (Pecho-Vrieseling et al., 2009; Hippenmeyer et al., 2005; Kramer et al., 2006). ES cell recombinants were screened by Southern blot and PCR analysis as previously described by Pecho-Vrieseling et al. (2009), Hippenmeyer et al. (2005), and Kramer et al. (2006).

Mice

The following mouse strains were used in this study: *trkc* mutant (Klein et al., 1994); *PlexinD1* mutant (Gu et al., 2005); *PlexinD1-floxed* (Pecho-Vrieseling et al., 2009; Zhang et al., 2009); *Wnt1-Cre* (Danielian et al., 1998); *Sema3E* mutant (Pecho-Vrieseling et al., 2009); and *Olig2-Cre* (Sürmeli et al., 2011; Dessaud et al., 2007). In this study, we used wild-type or *PlexinD1*$^{flox/flox}$ mice as controls of *PlexinD1*$^{f/-}$*: Wnt1-Cre* 15) and *Sema3E*$^{-/-}$ mice.

In Situ Hybridization, Immunocytochemistry, and X-gal Staining

Digoxigenin (DIG)-labeled cRNA probes were used for in situ hybridization as described before by Schaeren-Wiemers and Gerfin-Moser (1993). In situ hybridization was performed on 16–20 μm cryosections according to standard protocols. Dual-color fluorescence in situ hybridization histochemistry was performed as described (Price et al., 2002; Yoshida et al., 2006). We used rabbit anti-Pv (Swant), rabbit-tetramethylrhodamine (Invitrogen), rabbit anti-GFP (Molecular Probes), guinea pig anti-vGlut1 (Chemicon), goat anti-Sema3E (Santa Cruz Biotechnology), and rabbit anti-PlexinD1 (Chauvet et al., 2007) antibodies. Immunocytochemistry was performed as described (Yoshida et al., 2006; Leslie et al., 2011). X-gal staining of spinal cord was performed according to standard protocol.

Anterograde and Retrograde Tracing Experiments

Rho-Dex (3,000 MW; Invitrogen) was injected into the particular muscles of E14.5–E15.5 embryos and then incubated in the presence of oxygen for 18 hr. Rho-Dex is transported from the muscles to cell bodies of proprioceptive sensory and motor neurons. After tissues were fixed and sectioned, mRNA expression of *Sema3E* and *PlexinD1* identified by in situ hybridization was compared with Rho-Dex expression identified by anti-rhodamine antibody (Invitrogen).

Sema3E-AP Fusion Protein Binding

AP-fusion protein binding to tissue sections was performed before (Gu et al., 2005; Yoshida et al., 2006).

Electrophysiological Analysis

Dissection of Spinal Cord

Spinal cords were dissected essentially as previously described by Mears and Frank (1997). Briefly, P5–P7 mice were anesthetized on ice, perfused with cold artificial cerebral spinal fluid (ACSF), decapitated, and transferred to a chamber containing cold circulating oxygenated (95% O_2/5% CO_2) ACSF. ACSF contained 252 mM sucrose, 2.5 mM KCl, 2 mM $MgCl_2$, 2 mM $CaCl_2$, 1.25 mM NaH_2PO_4, 26 mM $NaHCO_3$, 10 mM glucose, and 5 mM kynurenic acid (pH 7.4). Spinal cords were exposed by dorsal laminectomy, hemisected, and isolated. The inferior gluteal nerve and the bundle of nerves to Ham muscles in one hindlimb were dissected in continuity with the spinal cord and cut at the entrance of each muscle for stimulation. The spinal cords were positioned in recording chamber and perfused with oxygenated Krebs buffer containing 117 mM NaCl, 3.6 mM KCl, 2.5 mM $CaCl_2$, 1.2 mM NaH_2PO_4, 1.2 mM $MgCl_2$, 11 mM glucose, and 25 mM $NaHCO_3$ (pH 7.4). The inferior gluteal nerve and nerves to the Ham muscle were placed in tightly fitting glass suction electrodes for stimulation severally, and the preparation was gradually warmed to 26°C.

Intracellular Recording

Motor neurons were impaled with sharp glass micropipettes with a resistance of 70–150 MΩ filled with 2 M potassium acetate, 0.5% fast green, and 0.2 M lidocaine N-ethyl bromide (Sigma-Aldrich). Signals were acquired with an amplifier (MultiClamp 700B; Molecular Devices). The data were digitized with an analog-to-digital converter (Digidata 1440A; Molecular Devices), stored on a personal computer with a data acquisition program (Clampex version 10; Molecular Devices), and analyzed with a special software package

(Clampfit version 10; Molecular Devices). Glu and Ham motor neurons were identified by antidromic response from Glu and Ham sensory nerve stimulation, respectively. Only motor neurons with a resting potential below −55 mV were used for analysis. Stimulations were added with square pulses of 0.1 ms at 1.5 times the strength that evoked maximal monosynaptic response at 1 Hz using a stimulus isolator unit (S88X Dual Output Square Pulse Stimulator, SIU-C Constant Current Stimulus Isolatin Unit; Grass Technologies). For each motor neuron analyzed, 20 sequential traces were recorded and averaged offline. To minimize contamination of monosynaptic sensory-evoked EPSPs by antidromic action potentials in the motor neuron when recording homonymous responses, 0.2 M lidocaine N-ethyl bromide was added to electrode solution to block voltage-gated sodium channel activation. When using this strategy, antidromic responses were generally completely blocked within the first 20 min of the recording.

Data Analysis

Homonymous monosynaptic EPSP onset latencies refer to the time delay between the stimulation artifact and the onset of the earliest arising EPSP, and di- or polysynaptic EPSP onset latencies were measured between the stimulation artifact and the onset of the second component of EPSP in controls. The time window for monosynaptic EPSP onset latencies of Ham sensory nerve stimulation was defined as the mean latency of control ± 2 SD and confirmed by a jitter analysis for the onset latencies of individual traces recorded before averaging, as described previously by Pecho-Vrieseling et al. (2009) and Vrieseling and Arber (2006).

Extracellular Recording

After dissecting, cords were incubated at room temperature for 1 hr, and sciatic nerves were stimulated electrically (0.1 ms at 0.3–0.5 mA) via a Grass S8800 stimulator and Grass Isolation Unit. The recorded potential was amplified with a Preamplifier (Astro-Med; P55A. C) to Axon Digitizer (Axon 1440A). Traces were stored using pClamp software. Recorded traces were averages of 20 individual traces at 0.1 Hz. After first recording, recombinant Sema3E (5 nM; R&D Systems) or Fc protein (5 nM; R&D Systems) was added.

Quantification of vGlut1-Positive Synaptic Terminals

Vibratome sections were stained with anti-vGlut1 and anti-rhodamine and viewed on an LSM510 confocal microscope (Zeiss). 3D views were reconstructed and analyzed using the Imaris surface tool (Bitplane).

SUPPLEMENTAL INFORMATION

Supplemental Information includes five figures and can be found with this article online at http://dx.doi.org/10.1016/j.celrep.2013.10.005.

ACKNOWLEDGMENTS

We thank M. Mendelsohn, J. Kirkland, and B. Han for help in the generation of *Isl-Sema3E* mice. K. Campbell, F.J. Alvarez, B. Gebelein, C. Gu, A. Kania, T. Kuwajima, R. Matsuoka, M. Nakafuku, M. O'Donovan, and H. Umemori provided comments on the manuscript. Y.Y. was supported by grants from the March of Dimes Foundation (5-FY09-106) and NINDS (NS065048). K.K. was supported by JSPS Postdoctoral Fellowships for Research Abroad. T.M.J. is an HHMI Investigator and is supported by grants from NINDS, EU Framework Program 7, Project ALS, The Harold and Leila Mathers Foundation, and The Wellcome Trust. S.A. was supported by the Swiss National Science Foundation, an ERC advanced grant, the Kanton Basel-Stadt, EU Framework Program 7, and the Novartis Research Foundation.

Received: March 2, 2013
Revised: August 4, 2013
Accepted: October 2, 2013
Published: November 7, 2013

REFERENCES

Alvarez, F.J., Villalba, R.M., Zerda, R., and Schneider, S.P. (2004). Vesicular glutamate transporters in the spinal cord, with special reference to sensory primary afferent synapses. J. Comp. Neurol. *472*, 257–280.

Arber, S., Ladle, D.R., Lin, J.H., Frank, E., and Jessell, T.M. (2000). ETS gene Er81 controls the formation of functional connections between group Ia sensory afferents and motor neurons. Cell *101*, 485–498.

Betley, J.N., Wright, C.V., Kawaguchi, Y., Erdélyi, F., Szabó, G., Jessell, T.M., and Kaltschmidt, J.A. (2009). Stringent specificity in the construction of a GABAergic presynaptic inhibitory circuit. Cell *139*, 161–174.

Brown, A.G. (1981). Organization in the Spinal Cord (New York: Springer).

Chauvet, S., Cohen, S., Yoshida, Y., Fekrane, L., Livet, J., Gayet, O., Segu, L., Buhot, M.C., Jessell, T.M., Henderson, C.E., and Mann, F. (2007). Gating of Sema3E/PlexinD1 signaling by neuropilin-1 switches axonal repulsion to attraction during brain development. Neuron *56*, 807–822.

Clandinin, T.R., and Feldheim, D.A. (2009). Making a visual map: mechanisms and molecules. Curr. Opin. Neurobiol. *19*, 174–180.

Cohen, S., Funkelstein, L., Livet, J., Rougon, G., Henderson, C.E., Castellani, V., and Mann, F. (2005). A semaphorin code defines subpopulations of spinal motor neurons during mouse development. Eur. J. Neurosci. *21*, 1767–1776.

Danielian, P.S., Muccino, D., Rowitch, D.H., Michael, S.K., and McMahon, A.P. (1998). Modification of gene activity in mouse embryos in utero by a tamoxifen-inducible form of Cre recombinase. Curr. Biol. *8*, 1323–1326.

Dessaud, E., Yang, L.L., Hill, K., Cox, B., Ulloa, F., Ribeiro, A., Mynett, A., Novitch, B.G., and Briscoe, J. (2007). Interpretation of the sonic hedgehog morphogen gradient by a temporal adaptation mechanism. Nature *450*, 717–720.

Ding, J.B., Oh, W.J., Sabatini, B.L., and Gu, C. (2012). Semaphorin 3E-Plexin-D1 signaling controls pathway-specific synapse formation in the striatum. Nat. Neurosci. *15*, 215–223.

Doyle, M.W., and Andresen, M.C. (2001). Reliability of monosynaptic sensory transmission in brain stem neurons in vitro. J. Neurophysiol. *85*, 2213–2223.

Eccles, J.C., Eccles, R.M., and Lundberg, A. (1957). The convergence of monosynaptic excitatory afferents on to many different species of alpha motoneurones. J. Physiol. *137*, 22–50.

Frank, E., and Mendelson, B. (1990). Specification of synaptic connections between sensory and motor neurons in the developing spinal cord. J. Neurobiol. *21*, 33–50.

Gu, C., Yoshida, Y., Livet, J., Reimert, D.V., Mann, F., Merte, J., Henderson, C.E., Jessell, T.M., Kolodkin, A.L., and Ginty, D.D. (2005). Semaphorin 3E and plexin-D1 control vascular pattern independently of neuropilins. Science *307*, 265–268.

Hippenmeyer, S., Vrieseling, E., Sigrist, M., Portmann, T., Laengle, C., Ladle, D.R., and Arber, S. (2005). A developmental switch in the response of DRG neurons to ETS transcription factor signaling. PLoS Biol. *3*, e159.

Honda, C.N. (1995). Differential distribution of calbindin-D28k and parvalbumin in somatic and visceral sensory neurons. Neuroscience *68*, 883–892.

Inaki, M., Yoshikawa, S., Thomas, J.B., Aburatani, H., and Nose, A. (2007). Wnt4 is a local repulsive cue that determines synaptic target specificity. Curr. Biol. *17*, 1574–1579.

Iwamasa, H., Ohta, K., Yamada, T., Ushijima, K., Terasaki, H., and Tanaka, H. (1999). Expression of Eph receptor tyrosine kinases and their ligands in chick embryonic motor neurons and hindlimb muscles. Dev. Growth Differ. *41*, 685–698.

Klein, R., Silos-Santiago, I., Smeyne, R.J., Lira, S.A., Brambilla, R., Bryant, S., Zhang, L., Snider, W.D., and Barbacid, M. (1994). Disruption of the neurotrophin-3 receptor gene trkC eliminates la muscle afferents and results in abnormal movements. Nature *368*, 249–251.

Kramer, I., Sigrist, M., de Nooij, J.C., Taniuchi, I., Jessell, T.M., and Arber, S. (2006). A role for Runx transcription factor signaling in dorsal root ganglion sensory neuron diversification. Neuron *49*, 379–393.

Ladle, D.R., Pecho-Vrieseling, E., and Arber, S. (2007). Assembly of motor circuits in the spinal cord: driven to function by genetic and experience-dependent mechanisms. Neuron *56*, 270–283.

Leslie, J.R., Imai, F., Fukuhara, K., Takegahara, N., Rizvi, T.A., Friedel, R.H., Wang, F., Kumanogoh, A., and Yoshida, Y. (2011). Ectopic myelinating

oligodendrocytes in the dorsal spinal cord as a consequence of altered semaphorin 6D signaling inhibit synapse formation. Development *138*, 4085–4095.

Mears, S.C., and Frank, E. (1997). Formation of specific monosynaptic connections between muscle spindle afferents and motoneurons in the mouse. J. Neurosci. *17*, 3128–3135.

Osterhout, J.A., Josten, N., Yamada, J., Pan, F., Wu, S.W., Nguyen, P.L., Panagiotakos, G., Inoue, Y.U., Egusa, S.F., Volgyi, B., et al. (2011). Cadherin-6 mediates axon-target matching in a non-image-forming visual circuit. Neuron *71*, 632–639.

Pecho-Vrieseling, E., Sigrist, M., Yoshida, Y., Jessell, T.M., and Arber, S. (2009). Specificity of sensory-motor connections encoded by Sema3e-Plxnd1 recognition. Nature *459*, 842–846.

Price, S.R., De Marco Garcia, N.V., Ranscht, B., and Jessell, T.M. (2002). Regulation of motor neuron pool sorting by differential expression of type II cadherins. Cell *109*, 205–216.

Rose, H.J., and Metherate, R. (2005). Auditory thalamocortical transmission is reliable and temporally precise. J. Neurophysiol. *94*, 2019–2030.

Sanes, J.R., and Yamagata, M. (2009). Many paths to synaptic specificity. Annu. Rev. Cell Dev. Biol. *25*, 161–195.

Schaeren-Wiemers, N., and Gerfin-Moser, A. (1993). A single protocol to detect transcripts of various types and expression levels in neural tissue and cultured cells: in situ hybridization using digoxigenin-labelled cRNA probes. Histochemistry *100*, 431–440.

Shen, K., and Scheiffele, P. (2010). Genetics and cell biology of building specific synaptic connectivity. Annu. Rev. Neurosci. *33*, 473–507.

Sürmeli, G., Akay, T., Ippolito, G.C., Tucker, P.W., and Jessell, T.M. (2011). Patterns of spinal sensory-motor connectivity prescribed by a dorsoventral positional template. Cell *147*, 653–665.

Tripodi, M., Stepien, A.E., and Arber, S. (2011). Motor antagonism exposed by spatial segregation and timing of neurogenesis. Nature *479*, 61–66.

Vrieseling, E., and Arber, S. (2006). Target-induced transcriptional control of dendritic patterning and connectivity in motor neurons by the ETS gene Pea3. Cell *127*, 1439–1452.

Williams, M.E., de Wit, J., and Ghosh, A. (2010). Molecular mechanisms of synaptic specificity in developing neural circuits. Neuron *68*, 9–18.

Williams, M.E., Wilke, S.A., Daggett, A., Davis, E., Otto, S., Ravi, D., Ripley, B., Bushong, E.A., Ellisman, M.H., Klein, G., and Ghosh, A. (2011). Cadherin-9 regulates synapse-specific differentiation in the developing hippocampus. Neuron *71*, 640–655.

Yoshida, Y., Han, B., Mendelsohn, M., and Jessell, T.M. (2006). PlexinA1 signaling directs the segregation of proprioceptive sensory axons in the developing spinal cord. Neuron *52*, 775–788.

Zhang, Y., Singh, M.K., Degenhardt, K.R., Lu, M.M., Bennett, J., Yoshida, Y., and Epstein, J.A. (2009). Tie2Cre-mediated inactivation of plexinD1 results in congenital heart, vascular and skeletal defects. Dev. Biol. *325*, 82–93.

Zlatic, M., Li, F., Strigini, M., Grueber, W., and Bate, M. (2009). Positional cues in the *Drosophila* nerve cord: semaphorins pattern the dorso-ventral axis. PLoS Biol. *7*, e1000135.